

# How well can wavelet denoising improve the accuracy of computing fundamental matrices?

Qi Li  
Department of CIS  
University of Delaware  
qili@cis.udel.edu

Tao Li, Shenghuo Zhu  
Department of CS  
University of Rochester  
{taoli, zsh}@cs.rochester.edu

Chandra Kambhampettu  
Department of CIS  
University of Delaware  
chandra@cis.udel.edu

**Abstract:** The existence of noise is a serious obstacle for solving many computer vision problems. Computing fundamental matrix is a typical one. Motivated by the success of wavelet denoising technique in image processing, we study the interesting question: how well wavelet denoising can improve the accuracy of computing fundamental matrices? The answer to this question depends on two sub-questions: 1) What wavelets should be applied? 2) On what kind of images could wavelets be applied to improve accuracy of their fundamental matrix? The experiment results show that wavelet denoising is promising in computer vision as well as in image processing.

**Keyword:** Wavelet denoising, fundamental matrix, residue, epipolar geometry, feature point correspondence.

## 1 Introduction

A fundamental matrix between two views of a 3D object maps a 2D point in the first view to a line in the second view, and hence reduces search space of finding its corresponding point in second view from 2D image plane to 1D line. Because of this important role of fundamental matrices in 3D computer vision, many works haven't been done on computation of accurate fundamental matrices [9, 7, 5, 12].

The accuracy of computing fundamental matrices is essentially dependent on the accuracy of feature point correspondence (feature points are also called *corner points*). There are several factors which affect the accuracy of stereo point correspondence: resolution of cameras, texture of the surface of the scene or objects, affine distortion of the scene and illumination change occurred in wide baseline scenario [16, 15, 11, 3], and the inherit existing image noise [5, 12]. In this paper, we focus on the effect of noise. It is well known that the accuracy of computing fundamental matrices is very sensitive to noise having even small variances [5, 12].

Gaussian smoothing is a simple denoising method and it is widely used in computer vision algorithms [1, 2, 14]. However, Gaussian smoothing destroys the structure of im-

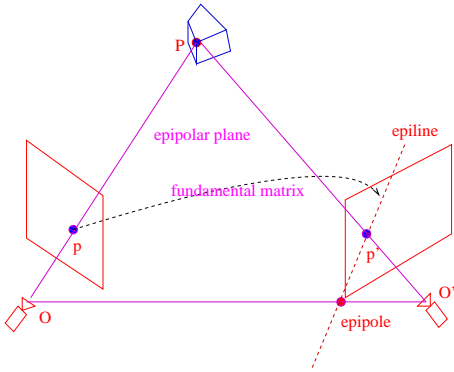
age data. In the feature point correspondence problem, there is a big tradeoff in deciding the length of Gaussian filter when Gaussian smoothing technique is involved. To reduce the effect of noise better, a longer Gaussian filter is preferred. While to preserve the structure of corner points, short Gaussian filter is desired. This disadvantage of Gaussian smoothing comes from the fact that Gaussian functions can not generate the basis of the underlying image data. The orthonormal basis property of wavelet brings the possibility of denoising without destroying the structure of input data [6, 8, 4].

Image processing researchers have already witnessed successes of wavelet denoising. However, it is not straightforward to claim that wavelet denoising must be successful and useful in computer vision research. The noise handled in image processing is usually of large variance [4] and the purpose of denoising in image processing is usually to improve the visual appearance of an image. While many computer vision algorithms are even sensitive to the noise with small variance and thus the purpose of denoising in computer vision is to improve the performance of computer vision algorithms. The questions, on what images wavelet can be applied, and what wavelets should be used are still open in computer vision.

In this paper, we are interested in investigating how useful the wavelet denoising technique is in improving the accuracy of computing fundamental matrices. The rest of this paper is organized as follows: In Section 2, we describe succinctly fundamental matrix and epipolar geometry. In Section 3, we present the basics of wavelet denoising. In Section 4, we compare wavelet denoising technique on images containing random information and those with no random information. Experiments on images Santa taken by our PVDV 400 camcorder and images from CMU stereo image dataset are given in Section 5. Conclusion and future work is given in Section 6.

## 2 Computing fundamental matrix and its residue

Fig. 1 shows an epipolar geometry for a 3D point  $P$  and two points  $O$  and  $O'$ , which are called the *optical centers* of two cameras. The plane determined by points  $P$ ,  $O$  and  $O'$  is called the *epipolar plane*. The line of intersection between the epipolar plane and image plane is called the *epipolar line* or *epiline*. There is another way to understand the epilines. The line  $\overline{OO'}$  intersects the image plane of the right camera at a point called the *epipole* of the right camera. The epilines associated with 3D point  $P$  in the image plane of  $O'$  is thus also the line that connects the epipole and the projected point of 3D point  $P$  in this image plane.



**Figure 1. An epipolar geometry of two views.**

The essence of the epipolar constraint is the *fundamental matrix*, which is a  $3 \times 3$  matrix that maps a point in one image plane to the corresponding epilines in another image plane. Formula (2.1) represents this relation.

$$[e_1 \ e_2 \ e_3]^T = F[p_x \ p_y \ 1]^T. \quad (2.1)$$

It is well known that seven corresponding points of two stereo images can determine a fundamental matrix. Assume that there are  $n \geq 7$  corresponding points  $(p_i, p'_i)$ . The following residue formula is used to evaluate the accuracy of a computed fundamental matrix:

$$\sum_{i=1}^n \left( \frac{1}{[Fp_i]_x^2 + [Fp_i]_y^2} + \frac{1}{[F^T p'_i]_x^2 + [F^T p'_i]_y^2} \right) (p_i'^T F p_i)^2. \quad (2.2)$$

It is straightforward to see that if the fundamental matrix is not accurate, a chosen feature point will be far away from its corresponding epilines, and so the amount of the residue will be large. More details on fundamental matrix and epipolar geometry can be found in [9, 5].

Because of the internal randomness of RANSAC algorithm [16, 10] in computing fundamental matrix, the result may not be exactly identical for different runs of the same

computation. In our following experiments, we will use the averaging strategy to compare the residues obtained from the images without and with wavelet denoising. More precisely, we compute the residues ten times in cases: without denoising and with denoising respectively and then choose the averages of each case.

## 3 Wavelet denoising – waveShrink

Suppose observation data  $y = (y_1, \dots, y_n)$  is a noisy realization of the signal  $x = (x_1, \dots, x_n)$ :

$$y_i = x_i + \epsilon_i, \quad i = 1, \dots, n, \quad (3.3)$$

where  $\epsilon_i$  is noise. A usual way to denoise is to find  $\hat{x}$  such that it minimizes the mean square error (MSE),

$$MSE(\hat{x}) = \frac{1}{n} \sum_{i=1}^n (\hat{x}_i - x_i)^2. \quad (3.4)$$

Donoho and Johnstone [8] developed a methodology called *waveShrink* for estimating  $x$ . It has been widely applied in many applications and implemented in commercial software, e.g., wavelet toolbox of Matlab [18].

There are three commonly used shrinkage functions: the hard, soft and the non-negative garrote shrinkage functions:

$$\begin{aligned} \delta_\lambda^H(x) &= \begin{cases} 0 & |x| \leq \lambda \\ x & |x| > \lambda \end{cases} \\ \delta_\lambda^S(x) &= \begin{cases} 0 & |x| \leq \lambda \\ x - \lambda & x > \lambda \\ \lambda - x & x < -\lambda \end{cases} \\ \delta_\lambda^G(x) &= \begin{cases} 0 & |x| \leq \lambda \\ x - \lambda^2/x & |x| > \lambda \end{cases} \end{aligned}$$

where  $\lambda \in [0, \infty)$  is the threshold.

Determining threshold  $\lambda$  is the key issue in waveShrink denoising. Minimax threshold is one of commonly used thresholds. The *minimax threshold*  $\lambda^*$  is defined as threshold  $\lambda$  which minimizes expression

$$\inf_{\lambda} \sup_{\theta} \left\{ \frac{R_\lambda(\theta)}{n^{-1} + \min(\theta^2, 1)} \right\}, \quad (3.5)$$

where  $R_\lambda(\theta) = E(\delta_\lambda(x) - \theta)^2, x \sim N(\theta, 1)$ . Interested readers can refer to [18] for other methods.

We will use the minimax threshold to denoise for two reasons. Firstly, minimax threshold method has been reported to be successful in processing different kind of data—signal, image, and medical/biological data [8, 17, 13]; Secondly, we are more interested in finding which classes of images wavelet denoising can help improving accuracy of epipolar geometry computation rather than trying to improve the accuracy of computing epipolar geometry for all kinds of images by testing all different thresholding rules. We think that the former goal is much more attainable than the latter one.

## 4 Images with random information and without random information

In this section, we have a brief discussion on the effect of random information contained in images when we apply wavelet denoising technique.

Fig. 2 shows two images of Santa, capped and non-capped. Fig. 3 (4) shows the intensity curves along row 20 (through cap region) in image of capped Santa (non-capped Santa respectively) without and with wavelet denoising. We see that the structure of intensity in capped Santa is changed after wavelet denoising while that in non-capped Santa is successfully preserved. The intuition behind this phenomenon is that information in cap region is typically random, so the wavelet denoising technique could not tell the noise from this random information. Therefore, we could expect the difference if we compute fundamental matrix on images with random information and images with little random information. In the former case, accuracy is expected to be degraded, while in the latter case, accuracy is expected to be improved.

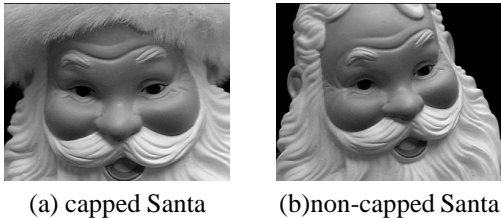


**Figure 2. Capped Santa contains random information in the cap region, whereas non-capped Santa contains little random information.**

## 5 Experiments

### 5.1 Epipolar geometry on capped Santa and non-capped Santa

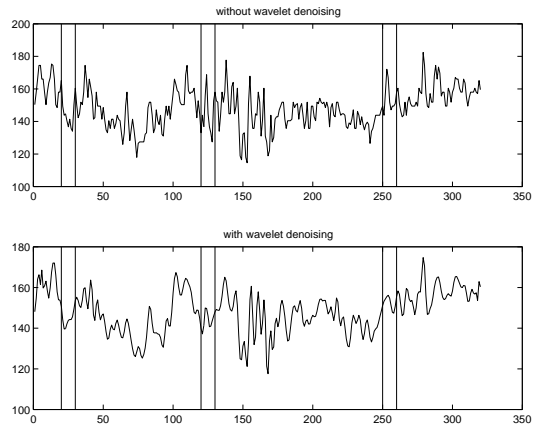
With less concern on choice of threshold (as what we discussed in Section 3), our remaining question is what kind of wavelet we should choose, wavelets with long supports<sup>1</sup> or wavelets with short supports? This question is similar to the question that how long the length of Gaussian filters should be chosen to smooth a given image [1].

Fig. 5 shows three different views of capped Santa (in the first row) and non-capped Santa (in the second row).

Fig. 6 illustrates that wavelets with longer supports can lead to more accurate computation<sup>2</sup> of fundamental matrix-

<sup>1</sup>Roughly speaking, support set means those intervals where the values of a wavelet function are not equal to zeros. Details can be found in [6].

<sup>2</sup>We compute fundamental matrices with image matching tool provided in INRIA website <http://www-sop.inria.fr/robotvis/demo/f-http/html/>.



**Figure 3. Intensity curves along row 20 in image of capped Santa without and with wavelet denoising. The structures of intensity in intervals [25 35], [120 130], [250 260] are seriously changed after wavelet denoising.**

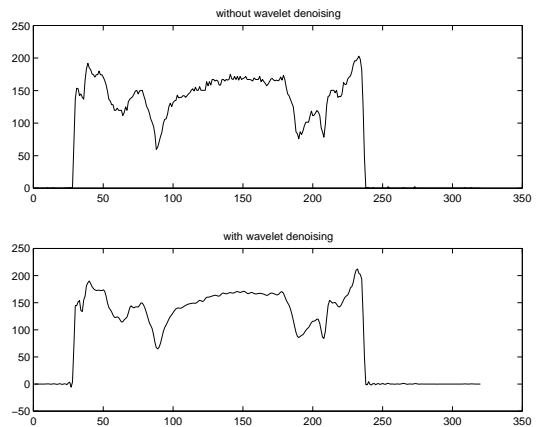


**Figure 4. Intensity curve along row 20 in image of non-capped Santa without and with wavelet denoising. The structure of intensity is preserved after wavelet denoising.**

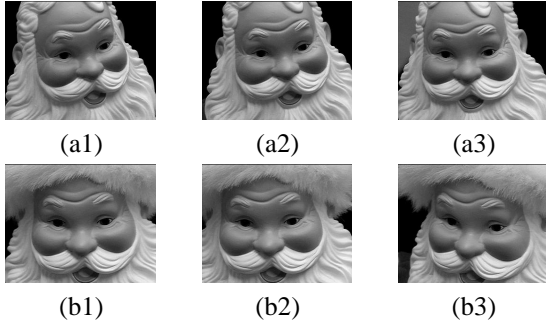


**Figure 5.** (a1)-(a3) are three different views of non-capped Santa; (b1)-(b3) are three different views of capped Santa.

ces than those with shorter supports do. In the following experiments, we keep on using wavelet db30 [6].

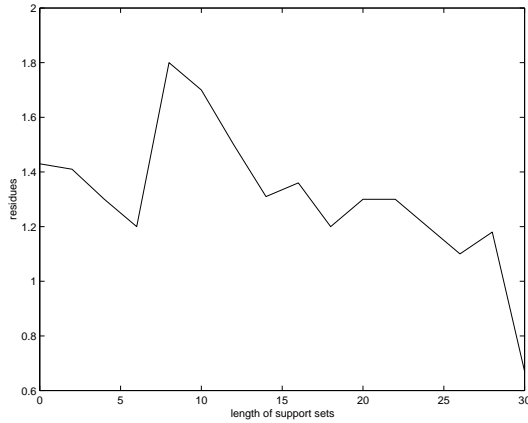


**Figure 6.** Residues by wavelets of increasing supports.

Table 1 shows the computed residues from three stereo pairs of non-capped Santa images and three stereo pairs of capped Santa images in cases: without denoising and with wavelet db30 denoising. We see that the accuracy of fundamental matrices of non-capped Santa images is always improved by wavelet denoising. Especially, the improvement in computing pair of view 2 and view 3 is essential. And the accuracy of fundamental matrices of capped Santa images are mainly degraded after wavelet denoising.

## 5.2 More experiments on CMU stereo image dataset

In this section, we report more experiment results on different images which are chosen from CMU stereo image dataset. They are images apple, arch, book, books, cart,

images	no denoising	db30 denoising
ncSanta (1,2)	1.06	0.98
ncSanta (1,3)	1.37	1.12
ncSanta (2,3)	1.43	0.67
cSanta (1,2)	1.05	1.15
cSanta (1,3)	1.19	1.40
cSanta (2,3)	1.14	0.96

**Table 1.** Residues are always decreased in non-capped Santa after wavelet denoising, while the residues are mainly increased in capped Santa after wavelet denoising; nc-Santa = non-capped Santa, and cSanta = capped Santa. (1,2) = (view 1, view 2), etc.

fruit, lab, mars, pentagon, pepsi and sandwich. Except images mars and pentagon, all other images are on indoor scene.

Table 2 shows the experiment results on CMU stereo images. The upper sub-table is of images on which wavelet denoising can help improving the accuracy of fundamental matrices and the lower sub-table is of images on which wavelet denoising degrades the accuracy of fundamental matrices.

images	no denoising	db30 denoising
arch	1.39	1.14
book	0.54	0.41
books	1.13	1.11
cart	1.16	0.66
lab	6.4e-14	1.24e-14
mars	1.40	1.05
pepsi	0.41	0.39
apple	0.65	0.71
pentagon	0.84	0.96
fruit	0.85	0.98
sandwich	2.1	2.2

**Table 2.** Residues in computing fundamental matrix of images in upper table are increased and in lower table are decreased; Wavelet denoising improves the accuracy of fundamental matrix for images without random information whereas decreases accuracy for images with random information.

The scene of images, apple, pentagon and sandwich contain random information. So wavelet denoising will destroy some real information in these images and degrade the accuracy of fundamental matrix as well as the case of capped Santa.

The degraded accuracy of fundamental matrix on images fruit is unexpected since image fruits do not contain random information. We observe that the number of matched points found in images fruit is more than 600 in both no denoising and with denoising cases while those found in other images is at most around 450. The reason is due to the highly regular texture in images fruit. The regular texture and large amount feature points increase the chance of mismatching. The experiments show that wavelet denoising increases the chance of mismatching when the texture is highly regular, so leads to the degraded accuracy of fundamental matrix.

Final observation is that indoor or outdoor scene is not a factor to determine whether wavelet denoising can be successful in improving the accuracy of fundamental matrix. Since the light source for indoor scene and outdoor scene are completely different, it is possible that the structure of image noise in indoor scene image is also different from that in outdoor scene, which may lead to different result when we apply wavelet denoising technique to them. However, in Table 2, the successful cases include both indoor scene and outdoor scene (mars) and the unsuccessful cases also include indoor scene and outdoor scene (pentagon). Fig. 7/8 group the CMU images according to whether the accuracy of fundamental matrix is increased or not.

## 6 Conclusions and future work

In this paper, we study an interesting question of how well wavelet denoising can improve accuracy of fundamental matrix. We concentrate on looking for an answer along two sub-questions: 1) Whether the length of a wavelet's support affects the accuracy of computing fundamental matrix or not? 2) For what kinds of stereo images can wavelet denoising improve the accuracy of their fundamental matrix? The experiment results show that wavelet denoising can help improving accuracy of fundamental matrix on a large class of images while it is useless for the stereo images containing randomize information or highly regular texture information.

Even though residue is an important criterion to evaluate the accuracy of fundamental matrix, it is possible, in practice, that the fundamental matrix of small residue is not accurate (due to existence of mismatching points and coincidence that each feature point is close to a wrong epilines). Better evaluation method may involve 3D reconstruction technique, this is, reconstructing the 3D scene with the computed fundamental matrix, which will be our future work.

## References

- [1] S. Avidan and A. Shashua. Novel view synthesis in tensor space. In *Proc. IEEE CVPR*, pages 1034–1040, 1997.

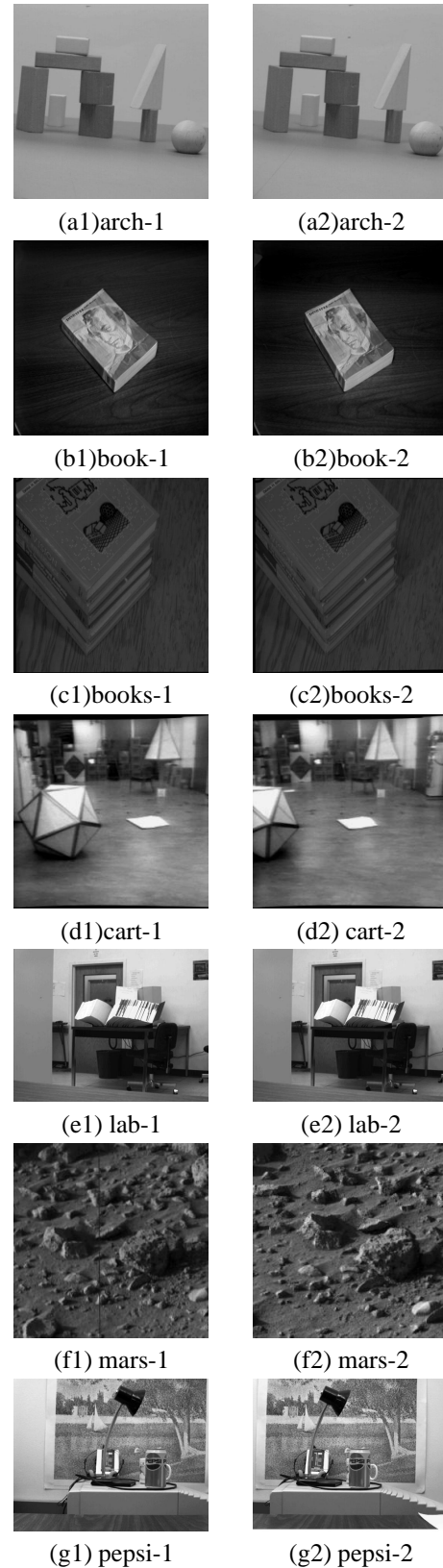
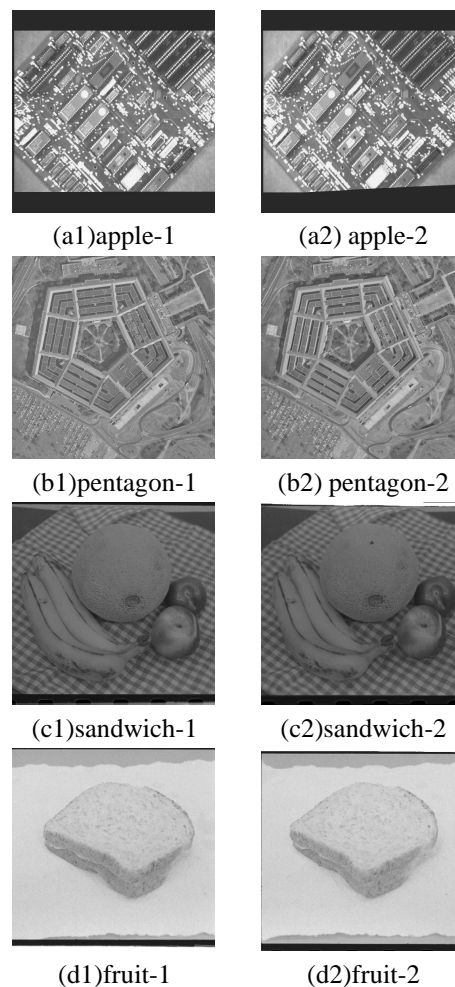


Figure 7. CMU images of improved accuracy with wavelet denoising.

- [2] J.L. Barron, D.J. Fleet, and S.S. Beauchemin. Performance of optical flow technique. *Intern. J. Comput. Vis.*, 12(1):43–77, 1994.
- [3] Adam Baumberg. Reliable feature matching across widely separated views. *preprint*.
- [4] S. Chang, B. Yu, and M. Vetterli. Spatially adaptive wavelet thresholding with context modeling for image denoising. In *ICIP*, volume 1, pages 535–539, 1998.
- [5] Gabriella Csurka, Cyril Zeller, Zhengyou Zhang, and Olivier D. Faugeras. Characterizing the uncertainty of the fundamental matrix. *Computer Vision and Image Understanding: CVIU*, 68(1):18–36, 1997.
- [6] I. Daubechies. Ten lectures on wavelets. SIAM, Philadelphia, 1992.
- [7] R. Deriche, Z. Zhang, Q.T. Luong, and O.D. Faugeras. Robust recovery of the epipolar geometry for an uncalibrated stereo rig. In *Proceedings of the ECCV*, pages 567–576. Springer-Verlag, May, 1994.
- [8] David L. Donoho and Iain M. Johnstone. Minimax estimation via wavelet shrinkage. *Annals of Statistics*, 26(3):879–921, 1998.
- [9] O.D. Faugeras. *Three-dimensional computer vision, a geometric viewpoint*. MIT Press, Cambridge, MA, 1993.
- [10] M.A. Fischler and R.C. Bolles. Random sample consensus: A paradigm for model fitting with application to image analysis and automated cartography. In *Graphics and image processing*, pages 381–395.
- [11] V. Gouet, P. Montesinos, and D. Pele. A fast matching method for color uncalibrated images using differential invariants. In *Proceedings of the British Machine Vision Conference*, pages 367–376, 1998.
- [12] R.I. Hartley. In defense of the eight-point algorithm. *IEEE Trans. on PAMI*, 19(6):580–593, 1997.
- [13] Qi Li, Tao Li, Shenghuo Zhu, and Chandra Kambhamettu. Improving medical/biological data classification performance by wavelet pre-processing. In *The IEEE International Conference on Data Mining, Maebashi City, Japan, Dec. 9-12, 2002*.
- [14] Tony Lindeberg. Linear spatio-temporal scale-space. In *Proc Scale-Space'97: Scale-Space Theories in Computer Vision*, volume Springer LNCS vol 1252, pages 113–127, 1997.
- [15] F. Mindru, T. Moons, and L. Van Gool. Moment invariants for viewpoint and illumination independent recognition of planar color patterns. Technical report, 1998.
- [16] P. Pritchett and A. Zisserman. Wide baseline stereo matching. In *Proceedings (ICCV-98) IEEE International Conference on Computer Vision*, pages 754–759, 1998.
- [17] Sylvain Sardy. Minimax threshold for denoising complex signals with waveshrink. *IEEE Transactions on Signal Processing*, 48(4):1023–1028, 2000.
- [18] Hong ye Gao. Wavelet shrinkage denoising using the non-negative garrote. *Journal of Computational and Graphical Statistics*, 7(4):469–488, 1998.



**Figure 8. CMU images of decreased accuracy with wavelet denoising.**